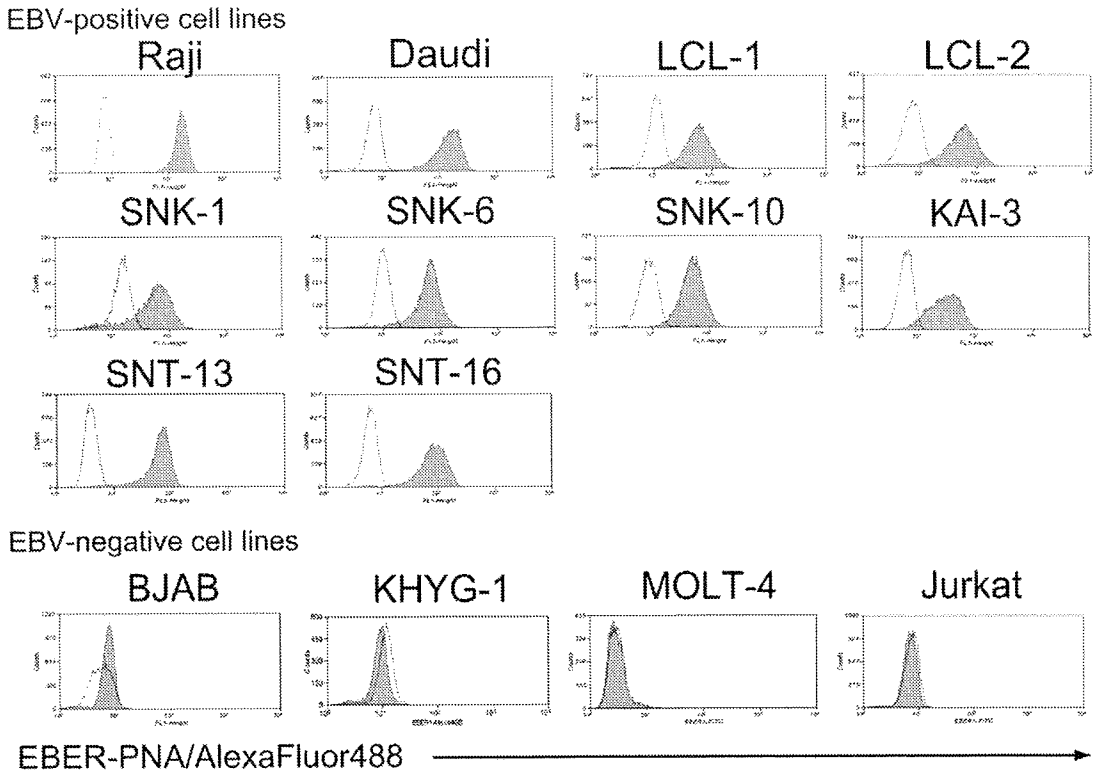

Figure 1. Detection of Epstein-Barr virus (EBV)–encoded small RNA (EBER) by flow cytometric in situ hybridization assay. EBV$^+$ or EBV$^-$ cells were fixed, permeabilized, and hybridized with either the EBER peptide nucleic acid (PNA) probe *(shaded histograms)* or the negative control PNA probe *(open histograms)*. After enhancement of fluorescent signals with Alexa Fluor 488–labeled antibodies, cells were analyzed by flow cytometry. Cell lines included the EBV$^+$ B cell lines, Raji, Daudi, lymphoblastoid cell line (LCL) 1, and LCL-2; EBV$^+$ natural killer (NK) cell lines, SNK-1, SNK-6, SNK-10, and KAI3; EBV$^+$ T cell lines, SNT-13 and SNT-16; EBV$^-$ B cell line, BJAB; EBV$^-$ NK cell line, KHYG-1; EBV$^-$ T cell lines, MOLT-4 and Jurkat. FITC, fluorescein isothiocyanate.

ever, biopsies are invasive and cannot always be performed, owing to the lack of nodal sites or difficulty of access. Because EBV-infected lymphocytes migrate in the peripheral blood in most EBV-associated lymphomas or lymphoproliferative diseases, peripheral blood lymphocytes can be examined instead of tissue specimens [7]. For this reason, applying EBER ISH to peripheral blood would allow EBV-infected cells to be identified and quantified using a more convenient and less invasive procedure.

Peptide nucleic acid (PNA) is a DNA/RNA analog capable of binding to DNA and RNA in a sequence-specific manner [10]. In PNA, nucleobases are attached to a backbone that consists of repetitive units of N-(2-aminoethyl)glycine, in contrast to the sugar-phosphate backbone of DNA/RNA. Because of the high binding affinity of PNA to DNA/RNA and its stability [11, 12], PNA probes have been used for fluorescent ISH to determine telomere lengths at chromosome ends [13–15].

In this study, we established a novel ISH method to detect EBER$^+$ suspension cells with flow cytometry using a commercially available EBER PNA probe [16]. By enhancing fluorescence and photostability and modifying the fixation and hybridization steps, we successfully stained both EBER and surface antigens. With this novel flow cytometric ISH (FISH) method, we showed that EBV$^+$ $\gamma\delta$ T cells were present in the peripheral blood of patients with hydroa vacciniforme–like lymphoproliferative disease [17], which was defined as an EBV$^+$ cutaneous T cell lymphoproliferative disease that occurs in children [6, 18].

METHODS

Cell lines. The EBV$^+$ B cell lines included Raji and Daudi, both of which were derived from Burkitt's lymphoma tissue, and 2 lymphoblastoid cell lines transformed with B95–8 EBV. BJAB, an EBV$^-$ B cell line, was used as a negative control. The EBV$^+$ T cell lines included SNT-13 and SNT-16 [19], and the EBV$^+$ NK cell lines included SNK-1, -6, and -10 [19], and KAI3 [20]. These T and NK cell lines were derived either from patients with chronic active EBV infection or from T or NK cell lymphomas. MOLT-4 and Jurkat were used as EBV$^-$ T cell lines [21], and KHYG-1 was used as an EBV$^-$ NK cell line [22].

Patients and samples. Three patients with hydroa vaccini-

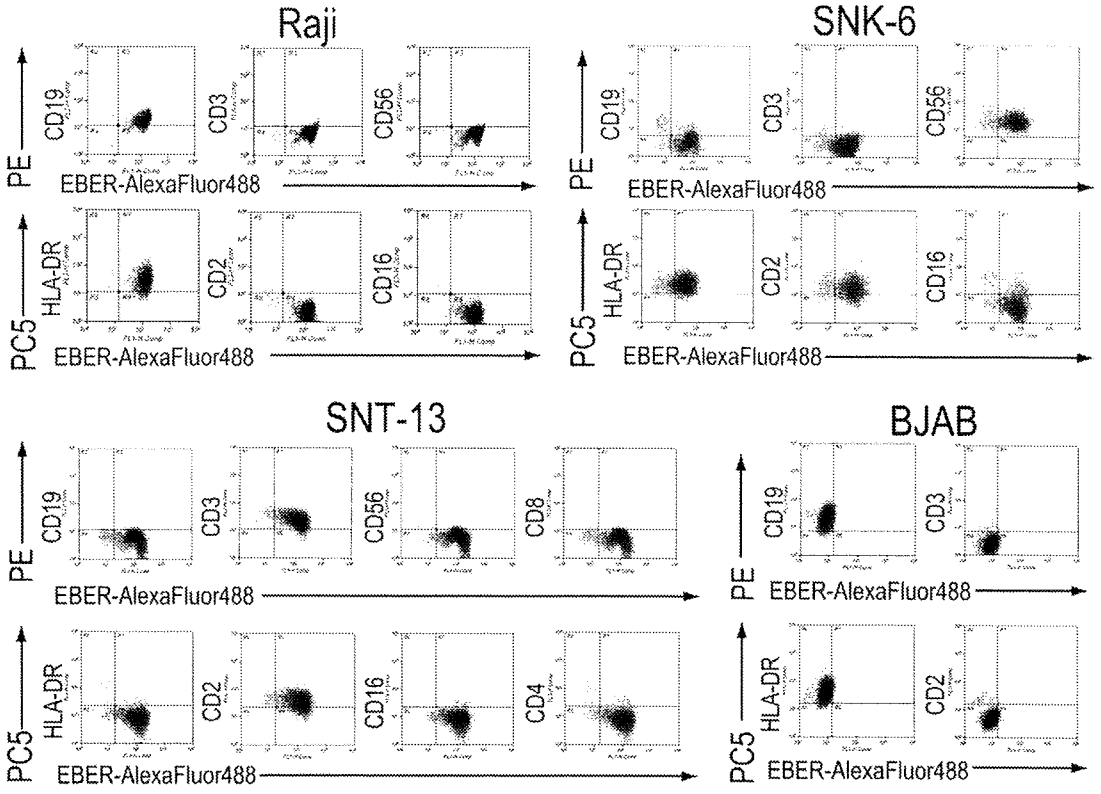

Figure 2. Dual staining for surface antigens and Epstein-Barr virus (EBV)–encoded small RNA (EBER) by flow cytometric in situ hybridization assay. Cells were stained for surface antigens with phycoerythrin (PE)– or PE–cyanin 5 (PC5)–labeled monoclonal antibodies and then fixed, permeabilized, and hybridized with the EBER peptide nucleic acid probe. After enhancement of fluorescent signals, cells were analyzed by flow cytometry. The EBV^+ B cell line was Raji; the EBV^+ natural killer (NK) cell line, SNK-6; the EBV^+ T cell line, SNT-13; and the EBV^- B cell line, BJAB.

forme–like lymphoproliferative disease and 1 patient with post-transplantation lymphoproliferative disease were enrolled in the study. As negative controls, 5 healthy volunteers who were seropositive for EBV were also enrolled. Heparinized blood samples were obtained, and peripheral blood mononuclear cells (PBMCs) were separated by density gradients. PBMCs were cryopreserved at −80°C until analysis.

Informed consent was obtained from all patients or guardians and healthy carrier donors. The institutional review board of Nagoya University Hospital approved the use of all specimens examined in this study.

Surface marker staining. Cells were stained with phycoerythrin (PE)–labeled anti-CD3 (clone UCHT1; eBioscience), anti-CD8 (clone B9.11; Immunotech), anti-CD19 (clone HD37; Dako, and anti-CD56 (clone N901; Immunotech) monoclonal antibodies and PE–cyanin 5 (PC5)–labeled anti-CD2 (clone 39C1.5; Immunotech), anti-CD4 (clone 13B8.2; Immunotech), anti-CD16 (clone 3G8; Immunotech), anti-CD56 (clone N901; Immunotech), anti–HLA-DR (clone IMMU357; Immunotech), anti-$\alpha\beta$ T cell receptor (TCR) (clone IP26; eBioscience), and anti-TCR$\gamma\delta$ (clone IMMU510; Immunotech) monoclonal antibodies for 1 h at 4°C. Isotype-matched monoclonal mouse immunoglobulin (Ig) G antibodies were used in each experiment as controls.

PNA probes. The EBER PNA probe, Y5200, was purchased from Dako. The Y5200 probe is a mixture of 4 different fluorescein-labeled PNA probes complementary to EBER [16]. The negative control PNA probe (Dako), which consists of fluorescein-conjugated random PNA probes, was used as a negative control. The positive control PNA probe (Dako) directed against glyceralaldehyde 3-phosphate dehydrogenase was used as a positive control. Each PNA probe was labeled with fluorescein isothiocyanate (FITC).

FISH technique. The following experiments were performed in 1.5-mL microcentrifuge tubes (Corning). For surface marker staining, cells were stained with the appropriate antibodies before fixation and hybridization. Cultured cells (2×10^5) or PBMCs (5×10^5) were fixed with 1% (vol/vol) acetic acid in 4% paraformaldehyde/phosphate buffered saline (PBS) for 40 min at 4°C. After being washed once with PBS, cells were permeabilized in 50 μL of 0.5% Tween 20/PBS at room temperature. Formamide, buffer, and water were added to the cells in permeabilization buffer so that the final formamide and buffer concentrations were the same as the hy-

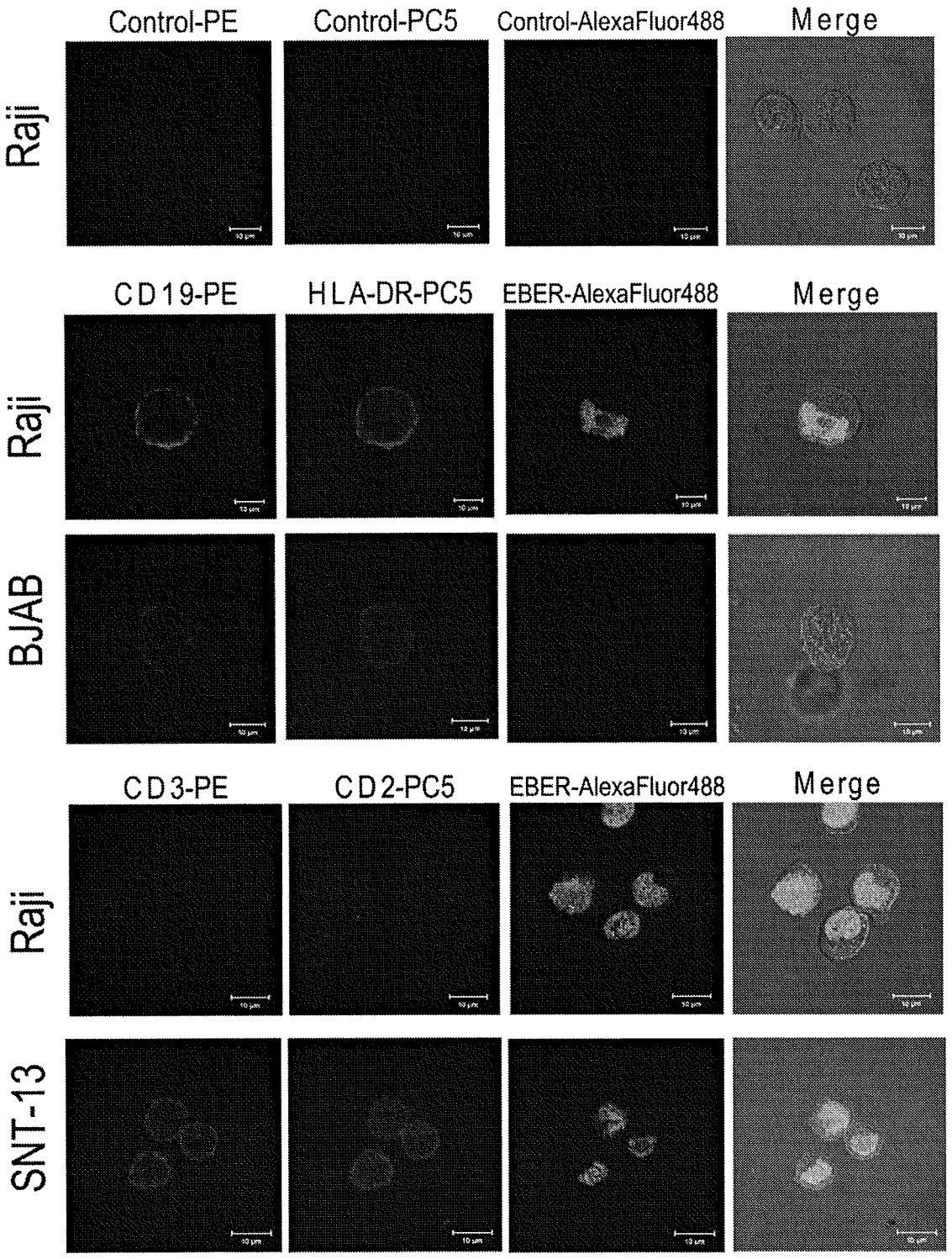

Figure 3. Detection of dual staining for surface antigens and Epstein-Barr virus (EBV)–encoded small RNA (EBER) by confocal microscopy. Cells were stained for surface antigens with phycoerythrin (PE)– or PE–cyanin 5 (PC5)–labeled monoclonal antibodies and then fixed, permeabilized, and hybridized with the EBER peptide nucleic acid probe. After enhancement of fluorescent signals, cells were mounted on glass slides and analyzed by confocal immunofluorescence microscopy. The EBV^+ B cell line was Raji; the EBV^- B cell line, BJAB; and the EBV^+ T cell line, SNT-13. Bars, 10 μm.

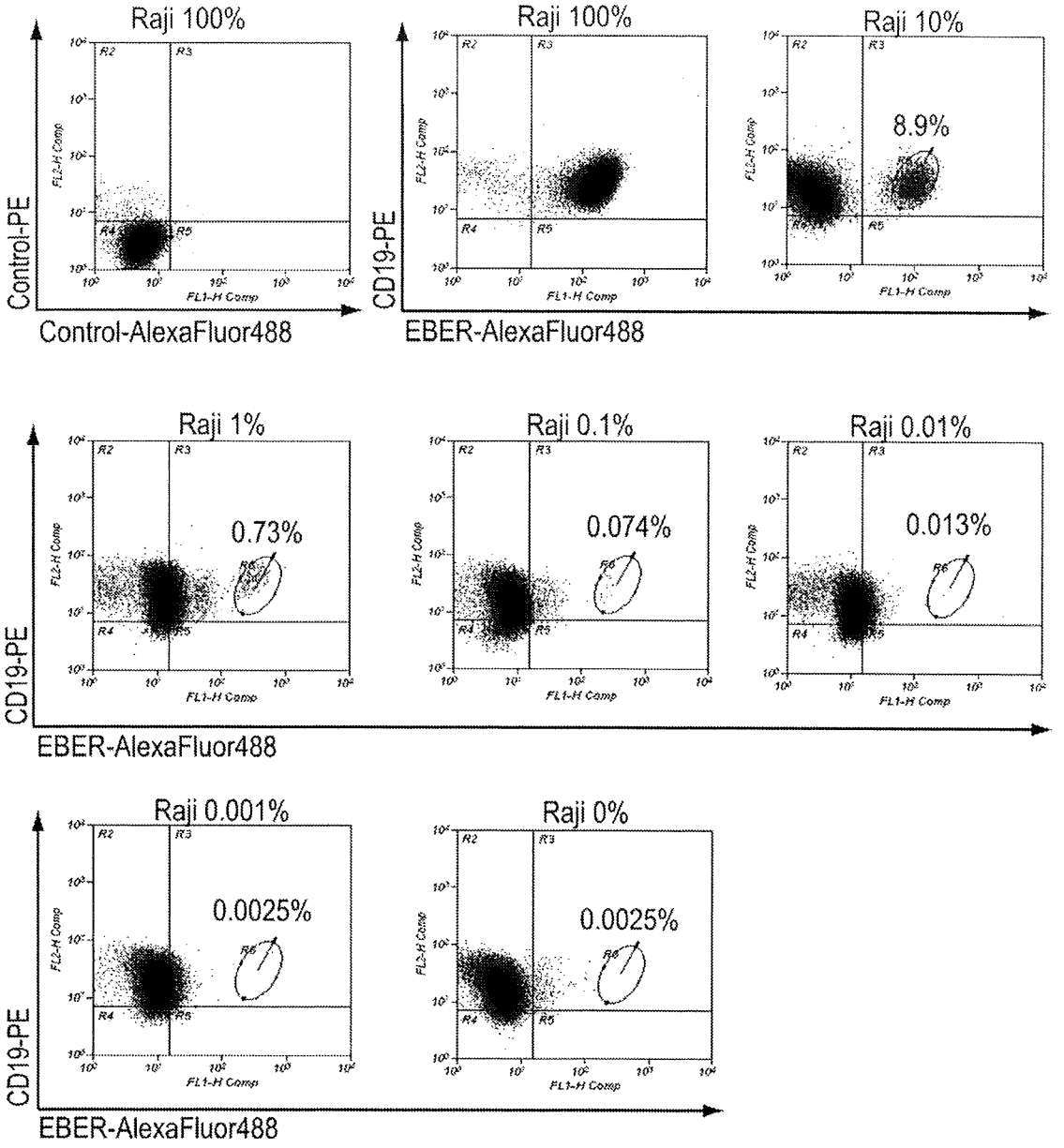

Figure 4. Minimum detection level of cells positive for Epstein-Barr virus (EBV) by flow cytometric in situ hybridization assay. EBV$^+$ Raji cells and EBV$^-$BJAB cells were mixed at various ratios, stained with phycoerythrin (PE)–labeled anti-CD19 antibody, and then fixed, permeabilized, and hybridized with the EBV-encoded small RNA (EBER) peptide nucleic acid (PNA) probe. After enhancement of fluorescent signals, the cells were analyzed by flow cytometry. The ratio of Raji to BJAB cells is shown above each quadrant. Numbers in quadrants indicate percentages of CD19$^+$EBER$^+$ cells.

bridization solution (6% [wt/vol] dextran sulfate, 10 mmol/L sodium chloride, 17.5% [vol/vol] formamide, 0.061% [wt/vol] sodium pyrophosphate, 0.12% [wt/vol] polyvinylpyrrolidone, 0.12% [wt/vol] Ficoll, 5 mmol/L disodium ethylenediaminetetraacetic acid, 50 mmol/L tris(hydroxymethyl) aminomethane [pH 7.5]). The cells were resuspended in 45 μL of hybridization solution containing 12 nmol/L of the EBER PNA probe, negative control PNA probe, or positive control PNA probe, all FITC labeled. Hybridization was carried out for 1 h at 56°C. Then cells were washed twice (for 10 and 30 min) with 0.5% Tween 20/PBS at 56°C. To enhance fluorescence and photostability, the Alexa Fluor 488 Signal Amplification Kit (Molecular Probes) was used. The kit protocol had 2 steps, using Alexa Fluor 488 rabbit anti-FITC to bind FITC-labeled probes and Alexa Fluor 488 goat anti-rabbit IgG for further enhancement.

Stained cells were analyzed using a FACSCalibur flow cytometer and CellQuest software, version 5.2.1 (Becton Dickinson). For cell lines, live gating was determined by forward

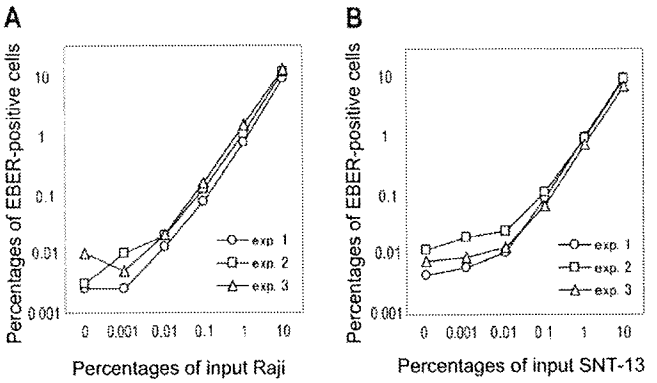

Figure 5. Correlation between the percentage of cells positive for Epstein-Barr virus (EBV)–encoded small RNA (EBER) and input EBV$^+$ cells. EBV$^+$ and EBV$^-$ cells were mixed at various ratios and analyzed by flow cytometric in situ hybridization assay. Each experiment (exp.) was done in triplicate. *A*, B cell lines included Raji (EBV$^+$) and BJAB (EBV$^-$). *B*, T cell lines included SNT13 (EBV$^+$) and Jurkat (EBV$^-$).

and side scatter profiles. For PBMCs, lymphocytes were gated by standard forward and side scatter profiles [23]. Up to 50,000 events were acquired for each analysis.

Confocal microscopy. Cells were resuspended in 20 μL of PermaFluor mounting medium (Thermo) and mounted onto glass slides with coverslips. Samples were examined under an LSM 510 confocal immunofluorescence microscope (Carl Zeiss) [24].

Analyses of EBV DNA. Viral load was examined in the PBMCs of all patients. DNA was extracted from 1×10^6 PBMCs using a QIAamp Blood Kit (Qiagen). Real-time quantitative polymerase chain reaction (PCR) with a fluorogenic probe was performed as described elsewhere [25]. The amount of EBV DNA was calculated as the number of virus copies per microgram of PBMC DNA or per milliliter of whole blood.

To determine which cells harbored EBV, PBMCs were fractionated into CD3$^+$, CD19$^+$, CD56$^+$, TCR$\alpha\beta^+$, and TCR$\gamma\delta^+$ cells using an immunobead method (IMag Cell Separation System; Becton Dickinson) with 97%–99% purity. The fractionated cells were analyzed by real-time quantitative PCR and compared with PBMCs [26]. The clonality of EBV was determined using Southern blotting with a terminal repeat probe, as described elsewhere [27].

Rearrangement of the TCR gene. TCR gene rearrangement was determined by multiplex PCR assays using the T Cell Gene Rearrangement/Clonality assay (InVivoScribe Technologies), which was developed and standardized in a European BIOMED-2 collaborative study [28, 29].

RESULTS

FISH assay to detect EBER. EBV$^+$ or EBV$^-$ cell lines were fixed, permeabilized, and hybridized with the EBER PNA probe or negative control PNA probe. After enhancement of fluorescent signals, cells were analyzed by flow cytometry. On the basis of flow cytometry, Raji cells had a significant increase in fluorescence intensity of the EBER PNA probe compared with the negative control PNA probe (Figure 1). Other EBV$^+$ B cell lines (Daudi, lymphoblastoid cell line [LCL] 1, and LCL-2) were consistently positive for EBER. In addition to B cell lines, NK cell lines (SNK-1, SNK-6, SNK-10, and KAI3) and EBV$^+$ T cell lines (SNT-13 and SNT-16) were also positive for EBER, whereas EBV$^-$ B cell (BJAB), NK cell (KHYG-1), and T cell (MOLT-4 and Jurkat) lines were negative for EBER.

Dual staining for surface antigens and EBER. To identify and characterize EBV-infected cells, surface lymphocyte antigens and nuclear EBER must be detected simultaneously. To this end, we first stained surface antigens with PE- or PC5-labeled monoclonal antibodies and then fixed and hybridized the cells with the EBER PNA probe. After enhancement of fluorescence intensity with Alexa Fluor 488 antibodies, both Alexa Fluor 488–labeled EBER and PE- or PC5-labeled surface antigens were detected by flow cytometry. As shown in Figure 2, the EBV$^+$ B cell line, Raji, was positive for Alexa Fluor 488–labeled EBER, PE-labeled CD19, and PC5-labeled HLA-DR, but negative for CD2, CD3, CD16, and CD56. In contrast, the EBV$^+$ NK cell line, SNK-6, was positive for EBER, CD2, CD56, and HLA-DR, but negative for CD3 and CD19. The EBV$^+$ T cell line, SNT-13, was positive for EBER, CD2, and CD3, but negative for CD16, CD19, CD56, and HLA-DR. The EBV$^-$ cell line BJAB was negative for EBER, but surface CD19 and HLA-DR antigens were detected (Figure 2).

The dual staining for surface antigens and EBER was further confirmed by confocal microscopy (Figure 3). PE-labeled CD19 and PC5-labeled HLA-DR were present on the surface of both Raji and BJAB cells, whereas Alexa Fluor 488–labeled EBER was specifically detected in the nucleus of Raji cells but not BJAB cells. In contrast, CD3 and CD2 were not present on the surface of Raji cells but were detected on the surface of the EBV$^+$ T cell line, SNT-13.

Sensitivity of the FISH assay in identifying EBV$^+$ cells. To determine the lower detection limit of the FISH assay for EBV$^+$ cells, we mixed EBV$^+$ Raji and EBV$^-$ BJAB cells in various ratios and analyzed them using the FISH assay (Figure 4). When 10% of Raji cells were mixed with 90% of BJAB cells, 8.9% of CD19$^+$EBER$^+$ cells could be separated from CD19$^+$EBER$^-$ cells using the FISH assay. Consistently, as the Raji/BJAB ratio decreased, the percentage of CD19$^+$EBER$^+$ cells also decreased. EBER$^+$ cells could be quantified down to a ratio of 1:10,000 (Raji, 0.01%, CD19$^+$EBER$^+$ cells, 0.013%), although the population of CD19$^+$EBER$^+$ cells was not so clear at this ratio. When 0.001% of Raji cells were mixed with BJAB cells, the percentage of CD19$^+$EBER$^+$ cells was almost equal to 100% of

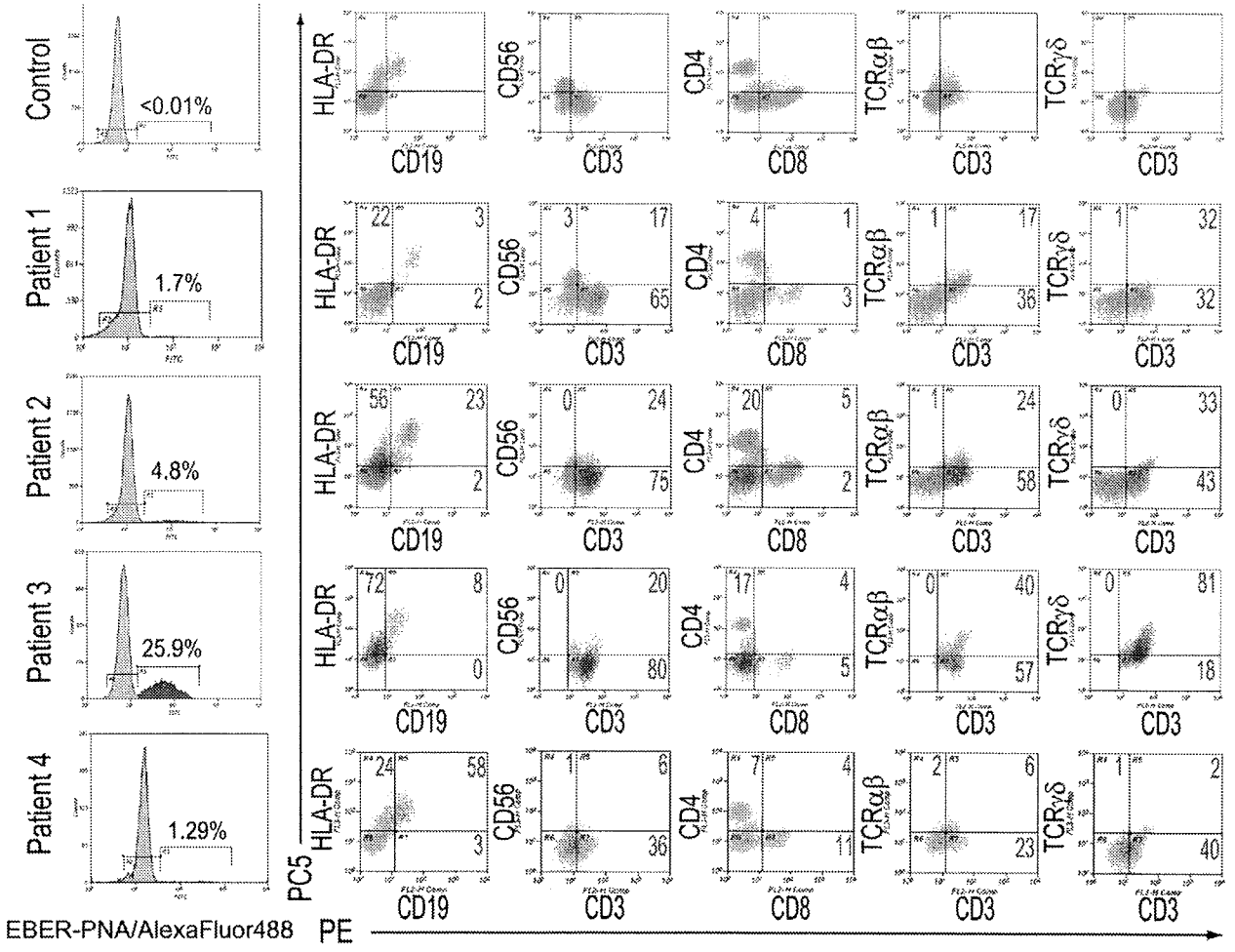

Figure 6. Quantification and identification of Epstein-Barr virus (EBV)–infected lymphocytes in patients with EBV-related lymphoproliferative diseases by flow cytometric in situ hybridization assay. Peripheral blood mononuclear cells were stained with phycoerythrin (PE)–labeled or PE–cyanin 5 (PC5)–labeled monoclonal antibodies and then fixed, permeabilized, and hybridized with the EBV-encoded small RNA (EBER) peptide nucleic acid (PNA) probe. After enhancement of fluorescent signals, the cells were analyzed by flow cytometry. Numbers in histograms represent percentages of EBER$^+$ lymphocytes in the total lymphocyte population. EBER$^+$ lymphocytes *(red)* and EBER$^-$ lymphocytes *(gray)* were gated and plotted on quadrants as PE-labeled and PC5-labeled surface antigens. Numbers in quadrants indicate percentages of EBER$^+$ cells for each surface immunophenotype. A healthy EBV-seropositive donor served as the control; patients 1–3 had hydroa vacciniforme–like EBV-associated T lymphoproliferative disease, and patient 4 had posttransplantation B cell lymphoproliferative disease. FITC, fluorescein isothiocyanate; TCR, T cell receptor.

BJAB cells (0.003% vs 0.003%), suggesting that the FISH assay was not quantitative at these ratios.

To confirm the accuracy and reproducibility of the FISH assay, we performed the mixing experiments (Raji, EBV$^+$ B cell line; BJAB, EBV$^-$ B cell line) 2 more times and additional mixing experiments (SNT13, EBV$^+$ T cell line; Jurkat, EBV$^-$ T cell line) in triplicate. The resulting correlations between the percentage of EBER$^+$ cells observed by FISH and the percentage of actual input EBV$^+$ cells are shown in Figure 5. These data show a clear correlation at 0.1%–10%, indicating that the assay was able to detect $\geq$0.1% of the EBV$^+$ cells accurately and reproducibly.

Application of the FISH assay to human PBMCs. PBMCs were obtained from 5 healthy volunteer donors and analyzed using the FISH assay. All donors were seropositive for EBV, but EBV DNA was not detected in their PBMCs by real-time PCR. Using the FISH assay, EBER$^+$ cells were not detected in any of the donors, whereas the positive control PNA probe directed against glyceralaldehyde 3-phosphate dehydrogenase was positive for all PBMCs (data not shown). Dual staining with antibodies to surface antigens and PNA probes showed that most lymphocyte markers were successfully detected and that distinct lymphocyte subsets could be separated, although some surface antigen intensities were not sufficient to separate certain populations (eg, CD56 and TCR$\alpha\beta$). A representative result is shown in Figure 6 (control).

Next, we applied the FISH assay to 3 patients with hydroa vacciniforme–like lymphoproliferative disease. These patients

Table 1. Clinical and Virologic Characteristics of Patients with Epstein-Barr Virus (EBV)–Associated Lymphoproliferative Diseases

Patient	Sex	Age, years	Age at onset, years	Diagnosis	EBV clonality	TCR gene rearrangement	EBV DNA, copies/μg DNA						EBV DNA, copies/mL whole blood
							PBMCs	$CD3^+$	$TCR\alpha\beta^+$	$TCR\gamma\delta^+$	$CD19^+$	$CD3^-CD56^+$	
1	M	16	5	Hydroa vacciniforme	Monoclonal	Vγ1f,Vγ10/Jγ,Vδ/Jδ	6100	16,380	8310	101,210	ND	860	11,850
2	M	11	5	Hydroa vacciniforme	Monoclonal	Vγ1f,Vγ10/Jγ,Vδ/Jδ	10,040	13,230	210	87,420	ND	240	ND
3	M	6	3	Hydroa vacciniforme	Monoclonal	Vδ/Jδ	41,760	46,730	6400	190,100	9090	6400	ND
4	M	6	6	PTLD	ND	ND	22,020	920	ND	ND	91,990	7290	47,660

NOTE. ND, not done; PBMCs, peripheral blood mononuclear cells; PTLD, posttransplantation lymphoproliferative disease; TCR, T cell receptor.

had no symptoms aside from photosensitivity and papulovesicular eruptions on their faces or arms. Skin biopsies were performed in patients 1 and 3. Small lymphoid cells without marked atypia infiltrated both the dermis and epidermis and were positive for EBER. These findings were compatible with hydroa vacciniforme–like lymphoproliferative disease, according to the World Health Organization classification [6]. The infiltrating cells were $CD3^+$ but $CD56^-$, indicating that they were T cells; further immunophenotyping for $TCR\alpha\beta$ and $TCR\gamma\delta$ was not performed. Extremely high amounts of EBV DNA with monoclonality were detected in the 3 patients' peripheral blood (Table 1). The clonality of the T cells was confirmed based on TCR gene rearrangement. Using the FISH assay, $EBER^+$ lymphocytes were detected in their PBMCs, with a frequency of 1.7% in patient 1, 4.8% in patient 2, and 25.9% in patient 3 (Figure 6). We repeated the FISH assay for patients 2 and 3 and obtained similar percentages of EBV^+ cells (patient 2, 5.0%; patient 3, 20.7%). $EBER^+$ lymphocytes were gated and plotted by PE-labeled surface antigens and PC5-labeled surface antigens. Most $EBER^+$ lymphocytes were $CD3^+CD4^-CD8^-TCR\gamma\delta^+$ T cells in the 3 patients examined. HLA-DR was expressed in $EBER^+$ lymphocytes from patients 2 and 3. To confirm these results, we applied an immunobead method to sort PBMCs into $CD3^+$, $TCR\alpha\beta^+$, $TCR\gamma\delta^+$, $CD19^+$, and $CD3^-CD56^+$ fractions and used quantitative real-time PCR to quantify EBV DNA in each fraction. The quantity of EBV DNA was high in the $CD3^+$ and $TCR\gamma\delta^+$ fractions but not in the $CD19^+$, $CD3^-CD56^+$, or $TCR\alpha\beta^+$ fractions (Table 1). For comparison, PBMCs from a patient with posttransplantation B cell lymphoproliferative disease were analyzed by both the FISH assay (Figure 6) and immunobead sorting, followed by EBV DNA quantification (Table 1). Both assays indicated that B cells in the peripheral blood of the patient were EBV^+, confirming the reliability of the FISH assay.

DISCUSSION

In this study, we established a novel FISH assay to directly quantify and simultaneously characterize EBV-infected lymphocytes using a commercially available EBER PNA probe. The probe is currently used to detect EBV-infected cells in formalin-fixed, paraffin-embedded tissue specimens. Just et al [16] also used this probe in a FISH assay. Crouch et al [30] used oligonucleotide probes directed against EBER in a FISH assay and succeeded in simultaneously detecting both EBER and surface antigens. However, both of these studies used FISH assays only with cell lines, and subsequent application to human PBMCs has not been reported. We preliminarily tested the EBER PNA probe with clinical specimens, but the fluorescence intensity of the probe was not sufficient to separate EBV^+ peripheral blood cells from EBV^- cells (data not shown). By enhancing fluorescence and photostability and modifying the fixation and hybridization steps, we successfully stained both EBER and surface antigens, not only in cell lines but also in human PBMCs. The order of immunophenotyping and ISH is important. We tried the reverse method (ISH preceded by surface immunophenotyping), but no surface antigens were detected by the monoclonal antibodies after ISH (data not shown).

This is a direct method to quantify EBV-infected cells and simultaneously characterize the infected cell phenotype, which helps not only to diagnose EBV-associated diseases but also to select monoclonal antibody–based therapy, such as anti-CD20 (rituximab) or anti-CD52 (Campath-1). We stained only surface lymphocyte markers in this study, but additional surface or intracellular molecules, such as cell adhesion markers, cytotoxic granules, or cytokines, will enable us to characterize and examine the function of EBV-infected lymphocytes. Furthermore, this method can be applied not only to peripheral blood but also to bone marrow and other body fluids, such as ascites, pleural effusions, and cerebrospinal fluid. In addition, FISH can be used for flow cytometric sorting of $EBER^+$ cells, which will further expand the ability to isolate and extensively study EBV-infected lymphocytes.

As a noninvasive method to diagnose and monitor EBV-associated lymphoproliferative diseases, measuring viral load in the peripheral blood is a necessary clinical tool. Quantitative PCR assays, such as real-time PCR, are the easiest and most reliable way to measure EBV load and are widely used for diagnosing and managing EBV-associated lymphoproliferative diseases, such as posttransplantation lymphoproliferative disease [7, 31–33]. The FISH assay has some disadvantages compared with quantitative PCR. First, the FISH assay has a lower sensitivity, although it can detect $\geq$0.1% of EBV-infected cells. Second, this assay cannot be applied to EBV-associated diseases

in which EBV-infected cells do not migrate into the peripheral blood, such as nasopharyngeal carcinoma or Hodgkin lymphoma [7, 34, 35]. Another unresolved problem with this assay is that after hybridization, the fluorescent signals of some surface antigens and antibodies were weak and cell separation was incomplete (eg, CD56 and TCR$\alpha\beta$ in Figure 6). We have not clarified this phenomenon completely, but we believe that antigen-antibody complexes were degraded or detached under the harsh hybridization conditions. The extent of this decrease in fluorescent signals differed among antibodies. We screened several monoclonal antibodies with different fluorochromes from different manufacturers for each surface antigen and then selected the best antibodies, as listed in Methods. Thus, selecting the appropriate antibody is important when performing the FISH assay. This problem may be overcome by using better antibodies, cross-linking antibodies or biotin-avidin enhancement, or modifying the fixation or hybridization steps, but the combination of antibodies and the hybridization conditions used in this study are sufficient to separate B, T, and NK cells from other populations.

Hydroa vacciniforme–like lymphoproliferative disease is an EBV$^+$ cutaneous malignancy associated with photosensitivity [6]. Although this condition is rare, it affects children and adolescents from Asia and Latin America [36–39]. It is characterized by a papulovesicular eruption that generally proceeds to ulceration and scarring. In some cases, systemic symptoms may be present, including fever, wasting, lymphadenopathy, and hepatosplenomegaly. In hydroa vacciniforme–like eruption, T cells with cytotoxic molecules often infiltrate the superficial dermis and subcutaneous tissues [39]. Most persons with this condition have clonal rearrangement of the TCR genes. EBV in these patients is also monoclonal, as shown terminal repeat analysis. These results indicate that clonal expansion of EBV-infected T cells causes the disease. However, the reported phenotypes of these T cells are variable, and both CD4$^+$ and CD8$^+$ T cell subsets have been reported [37, 40]. Most studies lack direct confirmation of these cell populations by double-staining with EBER and surface antigens.

In 3 patients with hydroa vacciniforme–like lymphoproliferative disease, we demonstrated that 1.7%–25.9% of peripheral lymphocytes were EBER$^+$ and that these lymphocytes were primarily CD3$^+$CD4$^-$CD8$^-$TCR$\gamma\delta^+$ T cells. This is the first study to determine the precise phenotype of EBV-infected lymphocytes in hydroa vacciniforme–like lymphoproliferative disease. $\gamma\delta$ T cells are the major T cell population in the epithelium of the skin and mucosa. They secrete various cytokines and have cytolytic properties [41]. It is possible that EBV-infected $\gamma\delta$ T cells play a central role in the formation of hydroa vacciniforme–like eruptions. The 3 patients examined in this study had no symptoms other than eruptions for several years (3–11 years), although they had a high percentage of clonal, EBV-infected lymphocytes in their peripheral blood. The prognosis of hydroa vacciniforme–like lymphoproliferative disease has been reported to be variable, and some cases do not progress for up to 10–15 years or seem to spontaneously enter remission [39, 42]. The 3 patients in our study may be exceptional and may not be representative of this patient population. Further investigation with a larger number of patients is needed to conclude that $\gamma\delta$ T cells are the primary EBV-infected cells in hydroa vacciniforme–like lymphoproliferative disease.

Hydroa vacciniforme–like eruption is also seen in severe chronic active EBV infection, which is caused by the clonal expansion of EBV-infected T or NK cells and seen mainly in East Asia [42–45]. These 2 conditions overlap, but their definitions are unclear [6, 46]. Because the 3 patients in the present study had only skin-restricted symptoms, they did not fulfil the classic criteria for chronic active EBV infection [47]. However, both severe chronic active EBV infection and hydroa vacciniforme–like lymphoproliferative disease develop in children and young adults from East Asia and may be caused by the clonal expansion of EBV-infected T or NK cells. To define and differentiate these diseases, additional data on EBV-associated lymphoproliferative diseases are needed. The FISH assay described in this study is a noninvasive, direct, and relatively convenient method to identify and characterize EBV-infected lymphocytes. With this novel method, we hope to further clarify the pathogenesis of EBV-associated lymphoproliferative diseases, including chronic active EBV infection, and to classify each disease more accurately.

Acknowledgments

We thank Tatsuya Tsurumi (Aichi Cancer Center) for the Raji and Daudi cell lines, Akihiro Tomita (Nagoya University Graduate School of Medicine) for the MOLT-4 and Jurkat cell lines, and Norio Shimizu (Tokyo Medical and Dental University) and Ayako Demachi-Okamura (Aichi Cancer Center) for the SNK-1, -6, and -10 and the SNT-13 and -16 cell lines. KAI3 and KHYG-1 were obtained from the Japanese Collection of Research Bioresources. We also thank Tom Just (Dako) for providing valuable comments regarding the FISH assay.

References

1. Straus SE, Cohen JI, Tosato G, Meier J. NIH conference. Epstein-Barr virus infections: biology, pathogenesis, and management. Ann Intern Med **1993**; 118:45–58.
2. Cohen JI. Epstein-Barr virus infection. N Engl J Med **2000**; 343:481–92.
3. Williams H, Crawford DH. Epstein-Barr virus: the impact of scientific advances on clinical practice. Blood **2006**; 107:862–9.
4. Rickinson AB, Kieff E. Epstein-Barr virus and its replication. In: Knipe DM, Howly PM, eds. Virology. 5th ed. Vol. 2. Philadelphia: Wolters Kluwer/Lippincott Williams & Wilkins, **2006**:2603–54.
5. Rickinson AB, Kieff E. Epstein-Barr virus. In: Knipe DM, Howly PM, eds. Virology. 5th ed. Vol. 2. Philadelphia: Wolters Kluwer/Lippincott Williams & Wilkins, **2006**:2655–700.
6. Quintanilla-Martinez L, Kimura H, Jaffe ES. EBV+ T-cell lymphoma of childhood. In: Swerdlow SH, Campo E, Harris NL, et al, eds. WHO

classification of tumours of haematopoietic and lymphoid tissues. 4th ed. Lyon: WHO Press, **2008**:278–80.
7. Kimura H, Ito Y, Suzuki R, Nishiyama Y. Measuring Epstein-Barr virus (EBV) load: the significance and application for each EBV-associated disease. Rev Med Virol **2008**; 18:305–19.
8. Randhawa PS, Jaffe R, Demetris AJ, et al. Expression of Epstein-Barr virus-encoded small RNA (by the EBER-1 gene) in liver specimens from transplant recipients with post-transplantation lymphoproliferative disease. N Engl J Med **1992**; 327:1710–4.
9. Middeldorp JM, Brink AA, van den Brule AJ, Meijer CJ. Pathogenic roles for Epstein-Barr virus (EBV) gene products in EBV-associated proliferative disorders. Crit Rev Oncol Hematol **2003**; 45:1–36.
10. Nielsen PE, Egholm M, Berg RH, Buchardt O. Sequence-selective recognition of DNA by strand displacement with a thymine-substituted polyamide. Science **1991**; 254:1497–500.
11. Egholm M, Buchardt O, Christensen L, et al. PNA hybridizes to complementary oligonucleotides obeying the Watson-Crick hydrogen-bonding rules. Nature **1993**; 365:566–8.
12. Demidov VV, Potaman VN, Frank-Kamenetskii MD, et al. Stability of peptide nucleic acids in human serum and cellular extracts. Biochem Pharmacol **1994**; 48:1310–3.
13. Lansdorp PM, Verwoerd NP, van de Rijke FM, et al. Heterogeneity in telomere length of human chromosomes. Hum Mol Genet **1996**; 5: 685–91.
14. Zijlmans JM, Martens UM, Poon SS, et al. Telomeres in the mouse have large inter-chromosomal variations in the number of T2AG3 repeats. Proc Natl Acad Sci USA **1997**; 94:7423–8.
15. Lansdorp PM. Telomeres, stem cells, and hematology. Blood **2008**; 111: 1759–66.
16. Just T, Burgwald H, Broe MK. Flow cytometric detection of EBV (EBER snRNA) using peptide nucleic acid probes. J Virol Methods **1998**; 73: 163–74.
17. Iwatsuki K, Xu Z, Takata M, et al. The association of latent Epstein-Barr virus infection with hydroa vacciniforme. Br J Dermatol **1999**; 140:715–21.
18. Nava VE, Jaffe ES. The pathology of NK-cell lymphomas and leukemias. Adv Anat Pathol **2005**; 12:27–34.
19. Zhang Y, Nagata H, Ikeuchi T, et al. Common cytological and cytogenetic features of Epstein-Barr virus (EBV)-positive natural killer (NK) cells and cell lines derived from patients with nasal T/NK-cell lymphomas, chronic active EBV infection and hydroa vacciniforme-like eruptions. Br J Haematol **2003**; 121:805–14.
20. Tsuge I, Morishima T, Morita M, Kimura H, Kuzushima K, Matsuoka H. Characterization of Epstein-Barr virus (EBV)-infected natural killer (NK) cell proliferation in patients with severe mosquito allergy: establishment of an IL-2-dependent NK-like cell line. Clin Exp Immunol **1999**; 115:385–92.
21. Sahai Srivastava BI, Minowada J. Terminal deoxynucleotidyl transferase activity in a cell line (molt-4) derived from the peripheral blood of a patient with acute lymphoblastic leukemia. Biochem Biophys Res Commun **1973**; 51:529–35.
22. Yagita M, Huang CL, Umehara H, et al. A novel natural killer cell line (KHYG-1) from a patient with aggressive natural killer cell leukemia carrying a p53 point mutation. Leukemia **2000**; 14:922–30.
23. Kuzushima K, Hoshino Y, Fujii K, et al. Rapid determination of Epstein-Barr virus-specific $CD8^+$ T-cell frequencies by flow cytometry. Blood **1999**; 94:3094–100.
24. Yamauchi Y, Kiriyama K, Kubota N, Kimura H, Usukura J, Nishiyama Y. The UL14 tegument protein of herpes simplex virus type 1 is required for efficient nuclear transport of the alpha transinducing factor VP16 and viral capsids. J Virol **2008**; 82:1094–106.
25. Kimura H, Morita M, Yabuta Y, et al. Quantitative analysis of Epstein-Barr virus load by using a real-time PCR assay. J Clin Microbiol **1999**; 37:132–6.
26. Kimura H, Hoshino Y, Hara S, et al. Differences between T cell-type and natural killer cell-type chronic active Epstein-Barr virus infection. J Infect Dis **2005**; 191:531–9.
27. Kimura H, Hoshino Y, Kanegane H, et al. Clinical and virologic characteristics of chronic active Epstein-Barr virus infection. Blood **2001**; 98:280–6.
28. van Dongen JJ, Langerak AW, Bruggemann M, et al. Design and standardization of PCR primers and protocols for detection of clonal immunoglobulin and T-cell receptor gene recombinations in suspect lymphoproliferations: report of the BIOMED-2 Concerted Action BMH4-CT98–3936. Leukemia **2003**; 17:2257–317.
29. Sandberg Y, van Gastel-Mol EJ, Verhaaf B, Lam KH, van Dongen JJ, Langerak AW. BIOMED-2 multiplex immunoglobulin/T-cell receptor polymerase chain reaction protocols can reliably replace Southern blot analysis in routine clonality diagnostics. J Mol Diagn **2005**; 7:495–503.
30. Crouch J, Leitenberg D, Smith BR, Howe JG. Epstein-Barr virus suspension cell assay using in situ hybridization and flow cytometry. Cytometry **1997**; 29:50–7.
31. Rooney CM, Loftin SK, Holladay MS, Brenner MK, Krance RA, Heslop HE. Early identification of Epstein-Barr virus-associated post-transplantation lymphoproliferative disease. Br J Haematol **1995**; 89:98–103.
32. Rowe DT, Webber S, Schauer EM, Reyes J, Green M. Epstein-Barr virus load monitoring: its role in the prevention and management of post-transplant lymphoproliferative disease. Transpl Infect Dis **2001**; 3:79–87.
33. Niesters HG. Molecular and diagnostic clinical virology in real time. Clin Microbiol Infect **2004**; 10:5–11.
34. Ambinder RF, Lin L. Mononucleosis in the laboratory. J Infect Dis **2005**; 192:1503–4.
35. Chan KC, Zhang J, Chan AT, et al. Molecular characterization of circulating EBV DNA in the plasma of nasopharyngeal carcinoma and lymphoma patients. Cancer Res **2003**; 63:2028–32.
36. Barrionuevo C, Anderson VM, Zevallos-Giampietri E, et al. Hydroa-like cutaneous T-cell lymphoma: a clinicopathologic and molecular genetic study of 16 pediatric cases from Peru. Appl Immunohistochem Mol Morphol **2002**; 10:7–14.
37. Chen HH, Hsiao CH, Chiu HC. Hydroa vacciniforme-like primary cutaneous CD8-positive T-cell lymphoma. Br J Dermatol **2002**; 147: 587–91.
38. Cho KH, Lee SH, Kim CW, et al. Epstein-Barr virus-associated lymphoproliferative lesions presenting as a hydroa vacciniforme-like eruption: an analysis of six cases. Br J Dermatol **2004**; 151:372–80.
39. Iwatsuki K, Satoh M, Yamamoto T, et al. Pathogenic link between hydroa vacciniforme and Epstein-Barr virus-associated hematologic disorders. Arch Dermatol **2006**; 142:587–95.
40. Doeden K, Molina-Kirsch H, Perez E, Warnke R, Sundram U. Hydroa-like lymphoma with CD56 expression. J Cutan Pathol **2008**; 35:488–94.
41. Kaufmann SH. gamma/delta and other unconventional T lymphocytes: what do they see and what do they do? Proc Natl Acad Sci U S A **1996**; 93:2272–9.
42. Nitta Y, Iwatsuki K, Kimura H, et al. Fatal natural killer cell lymphoma arising in a patient with a crop of Epstein-Barr virus-associated disorders. Eur J Dermatol **2005**; 15:503–6.
43. Kanegane H, Nomura K, Miyawaki T, Tosato G. Biological aspects of Epstein-Barr virus (EBV)-infected lymphocytes in chronic active EBV infection and associated malignancies. Crit Rev Oncol Hematol **2002**; 44:239–49.
44. Kimura H, Morishima T, Kanegane H, et al. Prognostic factors for chronic active Epstein-Barr virus infection. J Infect Dis **2003**; 187:527–33.
45. Katagiri Y, Mitsuhashi Y, Kondo S, Kanazawa C, Iwatsuki K, Tsunoda T. Hydroa vacciniforme-like eruptions in a patient with chronic active EB virus infection. J Dermatol **2003**; 30:400–4.
46. Ohshima K, Kimura H, Yoshino T, et al. Proposed categorization of pathological states of EBV-associated T/natural killer-cell lymphoproliferative disorder (LPD) in children and young adults: overlap with chronic active EBV infection and infantile fulminant EBV T-LPD. Pathol Int **2008**; 58:209–17.
47. Straus SE. The chronic mononucleosis syndrome. J Infect Dis **1988**; 157:405–12.